

# Distribution of zooplankton biomass and potential metabolic activities across the northern Benguela upwelling system

I. Fernández-Urruzola<sup>a</sup>, N. Osma<sup>a</sup>, T.T. Packard<sup>a</sup>, M Gómez<sup>a</sup> and L. Postel<sup>b</sup>

<sup>a</sup> Plankton Ecophysiology Group, Instituto de Oceanografía y Cambio Global, ULPGC, 35017, Canary Islands, Spain. E-mail: ifernandez@becarios.ulpgc.es  
<sup>b</sup> Zooplankton Ecology Group, Baltic Sea Research Institute, D-18119 Rostock, Warnemünde, Germany.

## INTRODUCTION

Upwelling ecosystems are among the most productive areas in the ocean. They mainly occur in the eastern boundaries, where the wind-driven divergence allows deep cold water masses to pump large amounts of nutrients into the sunlit layer. Both nutrient enrichment and light availability together, provide a suitable environment to sustain high biological productivity. However, the inherent variability of the oceanographic settings constrains the integrity of the biological communities on the order of days and affects the zooplankton physiology, which will ultimately control the efficiency of the net production. Zooplankton biomass and taxonomy were analyzed along a section off Namibian coast, while zooplankton respiration and  $\text{NH}_4^+$  excretion were assessed by measuring ETS and GDH activities, respectively. This enzymatic approach allowed a high data acquisition rate. Here we aimed to characterize, from an eulerian approach, how the physical structuring processes affected the biomass of zooplankton at 20°S within a matter of weeks, as well as to describe the magnitude of the impact that zooplankton metabolism has on the primary productivity.

## MATERIALS AND METHODS

### Study area

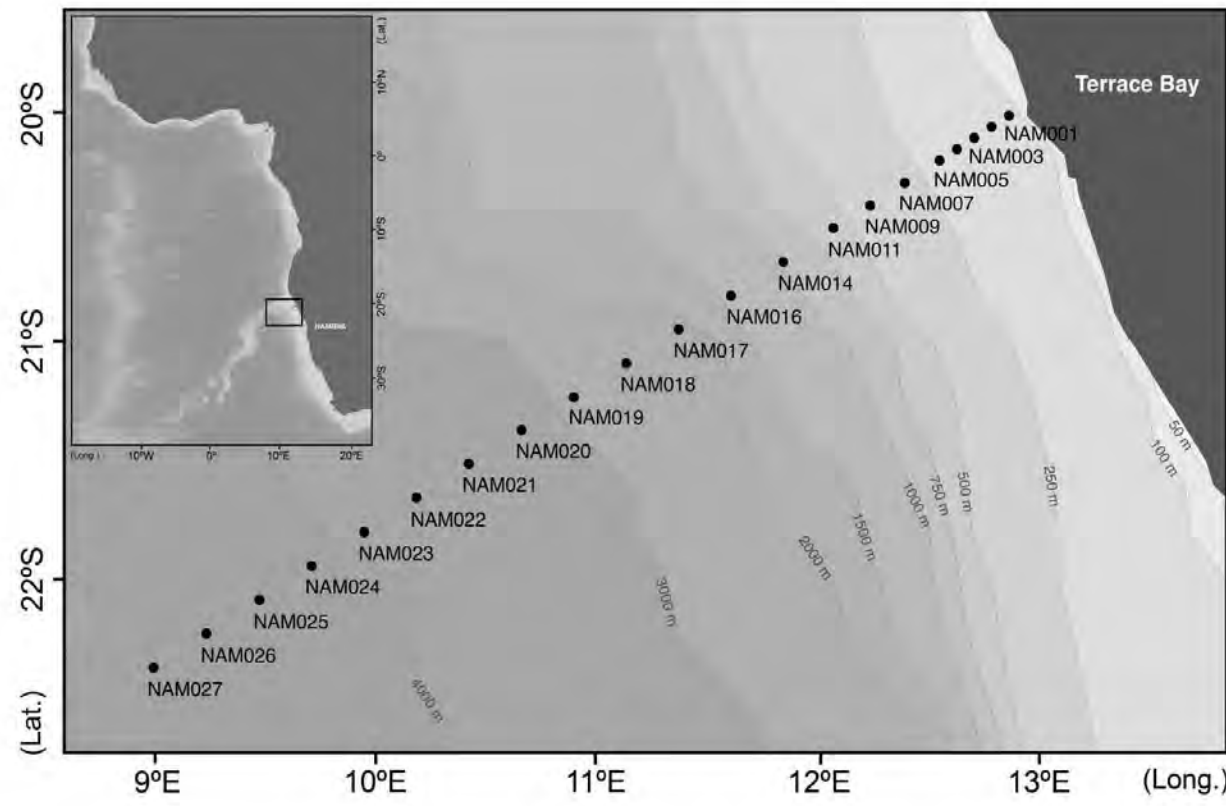
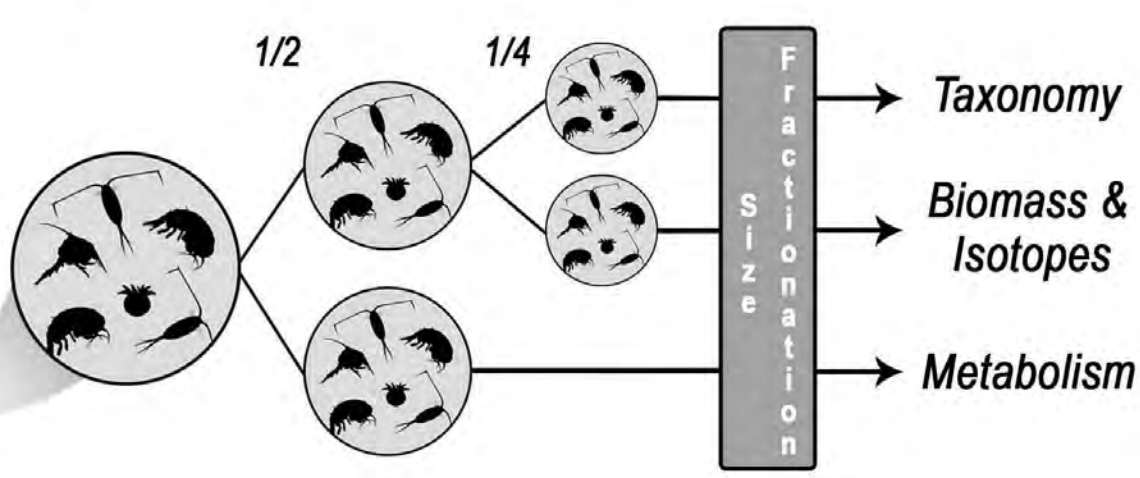


Fig. 1. Map of the study area showing the cross-shelf transect off Namibia. Stations from NAM001 to NAM018 were sampled four times, while samples from NAM019 to NAM027 were collected only once during the austral winter (August - September, 2011).

### Zooplankton sampling and analyses

Vertical Multinet hauls collecting zooplankton at three depth levels: 200-75 m, 75-25 m and 25-0 m.

#### SPLITTING



Samples were fractionated into 100-200  $\mu\text{m}$ , 200-500  $\mu\text{m}$ , 500-1000  $\mu\text{m}$  and >1000  $\mu\text{m}$  size classes prior storage.

### STORAGE AND LABORATORY WORK

#### Taxonomy

Samples stored in bottles filled with buffered formaldehyde (4%). Taxa determination by stereomicroscopy.

#### Biomass

Analyses of dry weight, carbon and nitrogen contents, as well as  $^{13}\text{C}$  and  $^{15}\text{N}$  isotopes on samples frozen at -20°C.

#### Metabolism

Samples ultrafrozen at -196°C for subsequent analyses of GDH and ETS activities.

## SUMMARY

The different water masses jointly with the biological forcing led to a shift in both the zooplankton community structure and biomass at 20°S. High respiratory and  $\text{NH}_4^+$  excretion rates were assessed for zooplankton, which paradoxically had a minor impact on the primary productivity of the northern Benguela waters.

## Acknowledgements



## RESULTS AND DISCUSSION

### Zooplankton biomass patterns

Zooplankton biomass was not distributed uniformly throughout the transect and underwent constant and rapid shifts in both temporal and spatial scales (Fig. 3) following the physical signature (not shown). The low biomass found in the newly upwelled neritic waters often yielded to a zooplankton gain over the shelf-break, characterized by the dominance of mature waters, in association with the offshore edge of the chlorophyll maxima (Fig. 2).

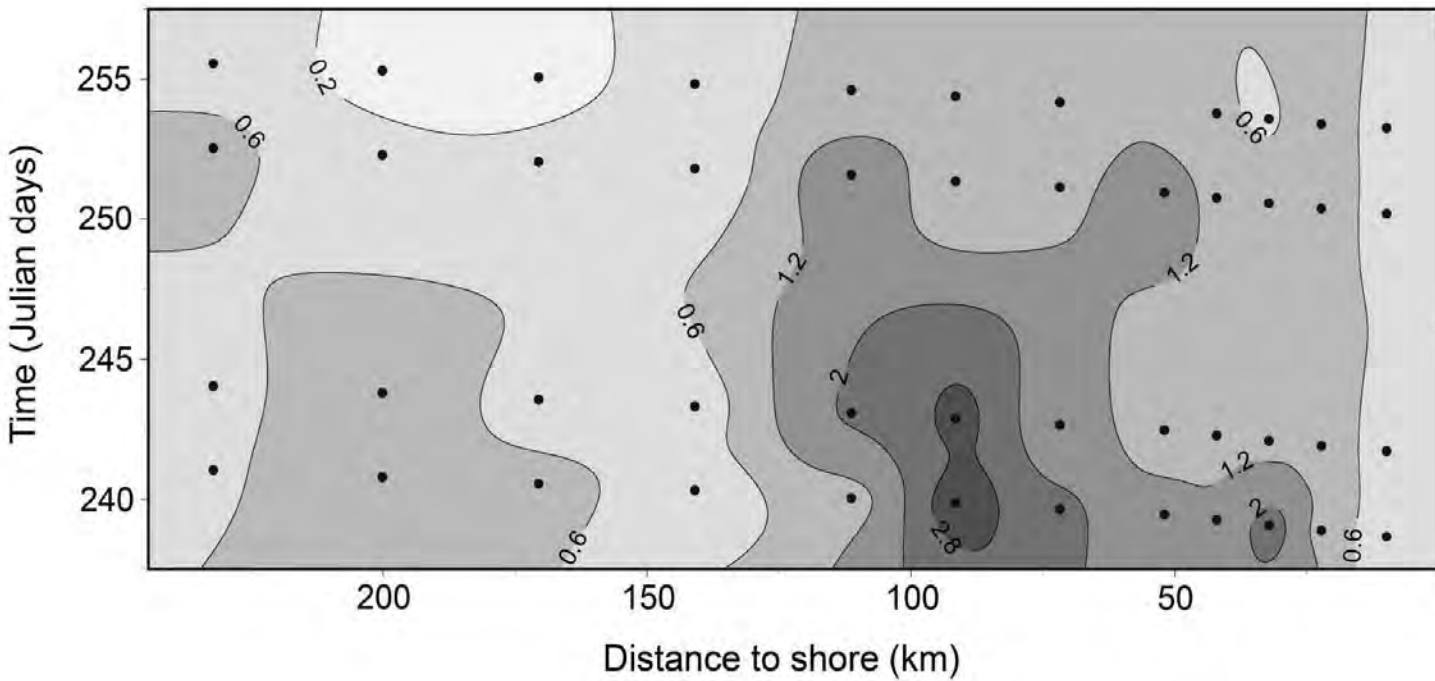


Fig. 3. Temporal variability of zooplankton biomass ( $\text{g DM m}^{-2}$ ) in the upper 25 m along the cross-shelf transect.

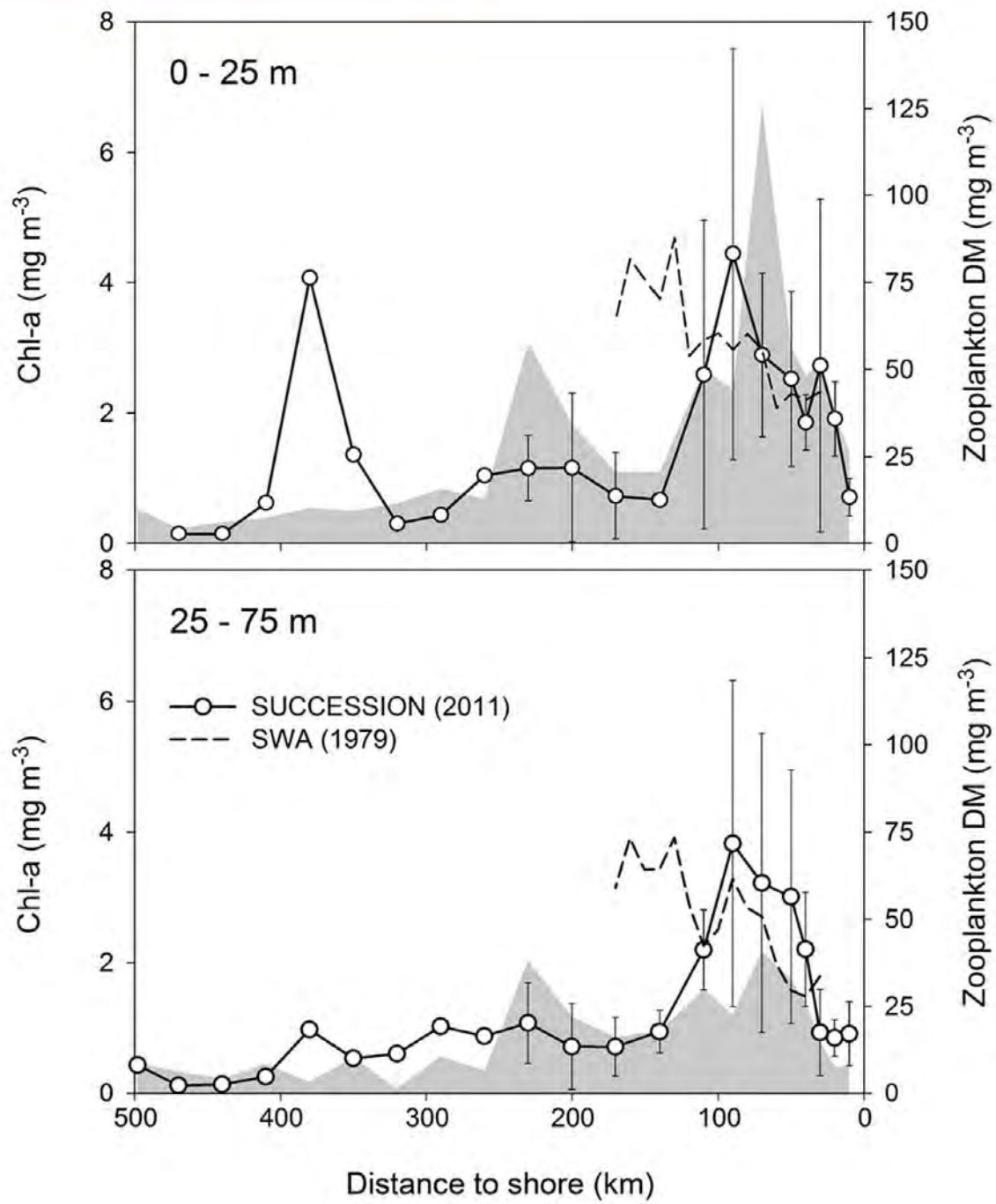


Fig. 2. Mean zooplankton biomass ( $\pm$  SD) at different depth levels with the chlorophyll concentrations given in grey.

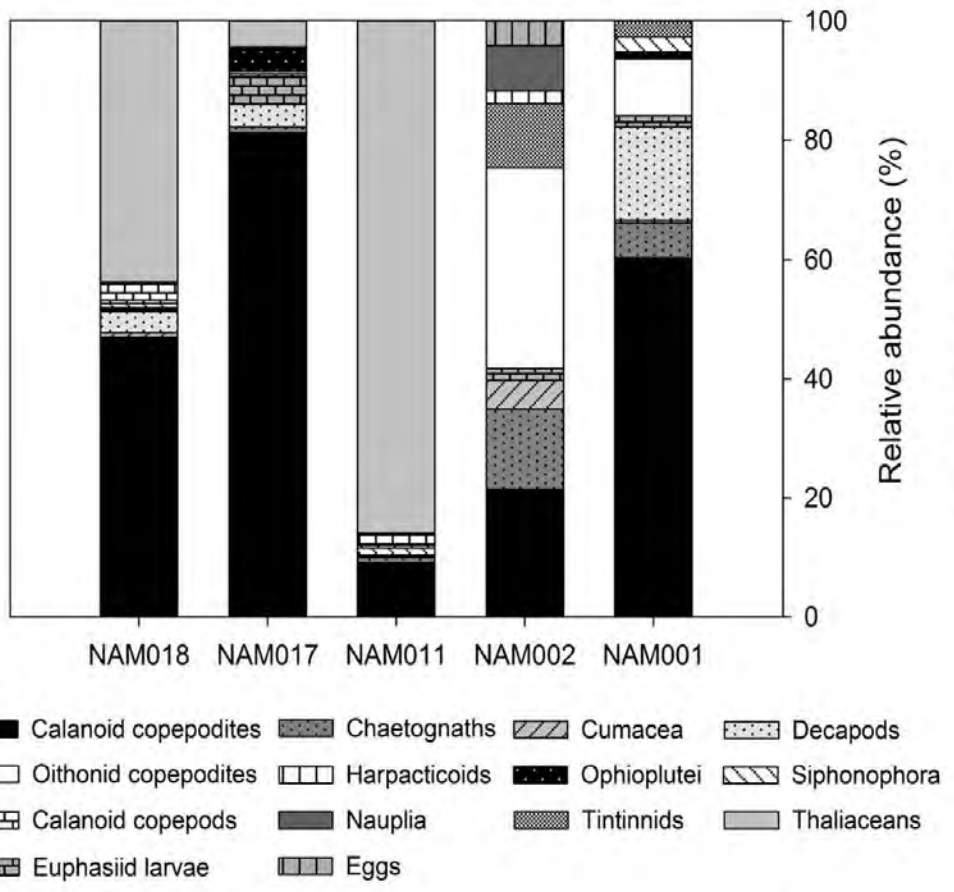


Fig. 4. Relative abundances of the taxa (>500  $\mu\text{m}$ ) which contributed with more than 2% to the zooplankton community.

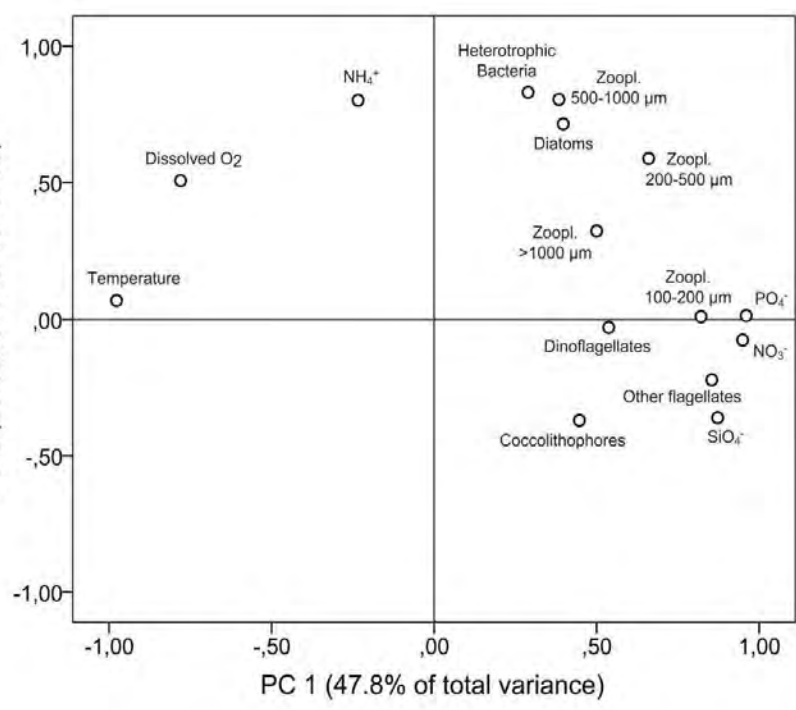


Fig. 5. Correlation matrix-based principal component analysis plot.

### Taxonomy and ecology

Overall, the zooplankton widely correlated with diatoms (Fig. 5), which argues for a bottom-up control over the trophic chain. The dominance of these chain-forming diatoms at the shelf-break might have entailed, however, a food particle-size limitation to the microzooplankton, which correlated more with the smaller flagellates. Despite copepods prevailing throughout the study area, their abundance dropped at the shelf-break as swarms of salps appear to have excluded other planktonic grazers (Fig. 4). All in all, the spatial pattern of zooplankton seem to be determined in the short-term not only by the complex interaction between mesoscale structures, but also by biological competition linked to the historical development of the water masses.

### Zooplankton metabolism

Even though the high averaged  $\text{O}_2$  consumption ( $112.4 \mu\text{mol O}_2 \text{ m}^{-3} \text{ d}^{-1}$ ) and  $\text{NH}_4^+$  excretion ( $10.3 \mu\text{mol NH}_4^+ \text{ m}^{-3} \text{ d}^{-1}$ ) rates, zooplankton respiration barely accounted for 5% of the gross primary production. Similarly, zooplankton community supported just a small fraction from the total production, which may highlight a major remineralization pathway through microheterotrophic processes.

Table 1. Percentages of gross primary production (GPP) both respired and regenerated by zooplankton in the upper 75 m of the water-column, and the resultant O/N ratio.

Station	GPP ( $\text{mmol C m}^{-2} \text{ d}^{-1}$ )	Zoop. Respiration ( $\text{mmol O}_2 \text{ m}^{-2} \text{ d}^{-1}$ )	% GPP <sub>resp</sub>	Zoop. $\text{NH}_4^+$ Excretion ( $\text{mmol NH}_4^+ \text{ m}^{-2} \text{ d}^{-1}$ )	% GPP <sub>Regen.</sub>	O/N
NAM001	75.80 ± 24.22	5.35 ± 2.11	6.08	0.45 ± 0.09	4.57	11.04 ± 8.65
NAM002	144.66 ± 14.29	8.42 ± 2.80	5.01	1.01 ± 0.11	5.33	10.25 ± 7.60
NAM003	145.45 ± 50.75	11.85 ± 7.14	7.01	0.95 ± 0.34	4.99	10.27 ± 7.44
NAM004	199.58 ± 37.25	14.84 ± 2.96	6.40	1.60 ± 0.60	6.11	12.24 ± 10.43
NAM005	216.73 ± 50.41	16.65 ± 12.25	6.61	1.74 ± 0.74	6.13	12.06 ± 7.15
NAM007	253.21 ± 48.92	16.53 ± 5.66	5.61	1.44 ± 0.58	4.33	14.47 ± 11.10
NAM009	248.02 ± 66.67	19.65 ± 13.94	6.81	1.55 ± 1.44	4.75	19.88 ± 13.16
NAM011	231.01 ± 27.09	11.21 ± 3.24	4.17	0.82 ± 0.19	2.70	15.09 ± 10.75
NAM014	128.67 ± 26.95	5.39 ± 1.50	3.60	0.98 ± 0.14	5.80	5.82 ± 2.00
NAM016	133.78 ± 16.04	3.76 ± 2.53	2.42	0.79 ± 0.35	4.51	4.54 ± 2.53
NAM017	181.26 ± 53.66	5.41 ± 4.00	2.57	0.93 ± 0.56	3.90	6.57 ± 3.75
NAM018	129.39 ± 39.41	7.27 ± 2.98	4.83	1.06 ± 0.43	6.22	7.06 ± 2.65
NAM019	101.45	8.21	6.97	1.60	12.04	5.33
NAM020	130.55	7.43	4.90	1.12	6.54	6.33
NAM021	110.67	2.64	2.05	0.61	4.19	4.84
NAM022	124.68	6.05	4.17	0.47	2.88	12.74
NAM023	103.23	10.45	8.71	1.25	9.26	8.58
NAM024	87.29	2.29	2.26	0.59	5.20	4.51
NAM025	80.07	0.90	0.97	0.22	2.13	5.58
NAM026	85.67	0.85	0.86	0.16	1.41	6.92
NAM027	103.27	-	-	-	-	-

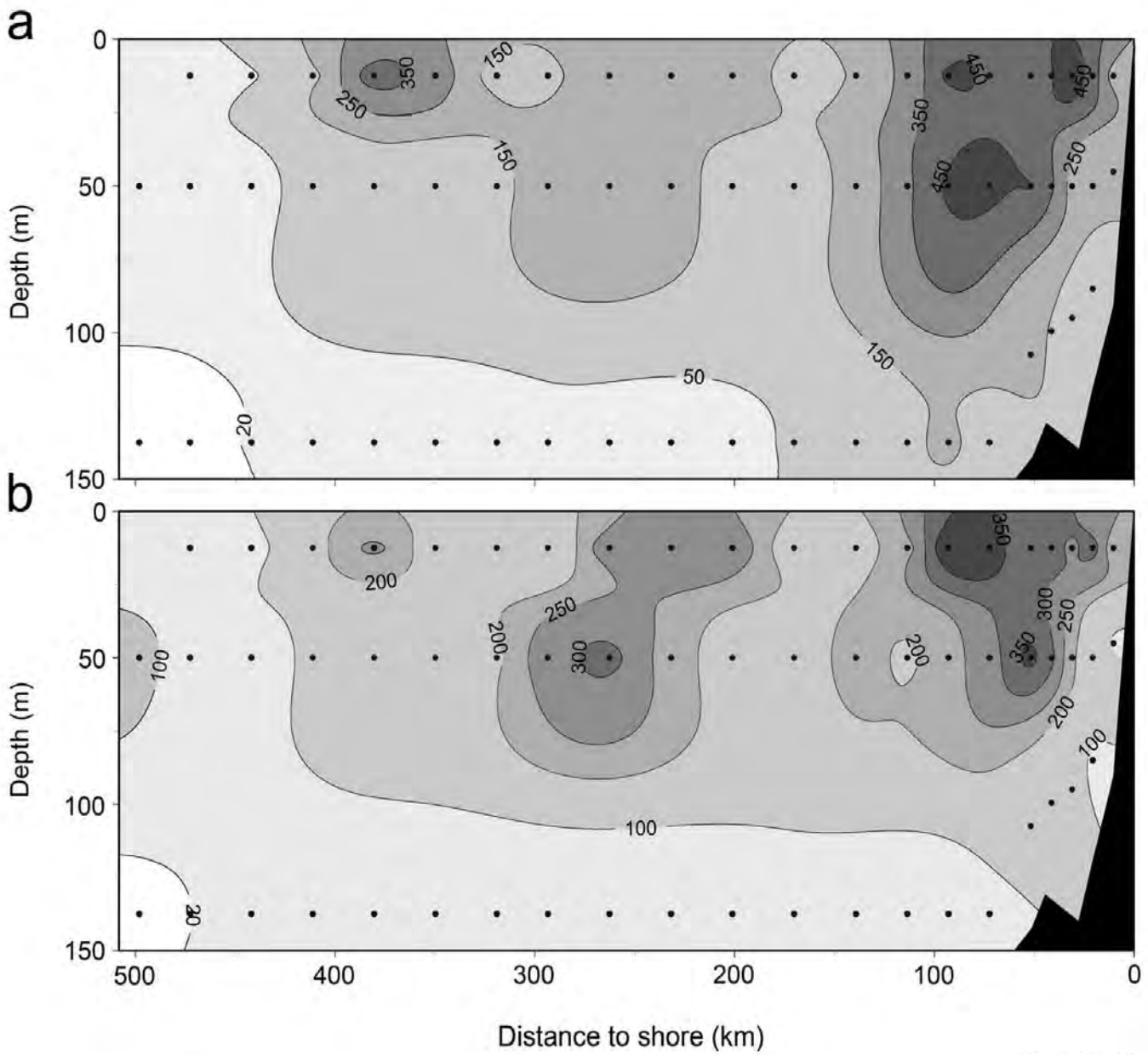


Fig. 6. (a) Averaged ETS activities ( $\mu\text{mol O}_2 \text{ m}^{-3} \text{ d}^{-1}$ ) and (b) GDH activities ( $\mu\text{mol NH}_4^+ \text{ m}^{-3} \text{ d}^{-1}$ ) profiles.

